

pubs.acs.org/crystal Article

# Triply-Reduced Hexa-peri-hexabenzocoronenes: Solid-State **Structures and Magnetic Properties**

Published as part of a Crystal Growth and Design virtual special issue on Molecular Magnets and Switchable Magnetic Materials

Zheng Zhou, Zheng Wei, Xuelin Yao, Xiao-Ye Wang, Klaus Müllen, Minyoung Jo, Michael Shatruk,\* and Marina A. Petrukhina\*



Cite This: Cryst. Growth Des. 2023, 23, 1189-1194



**ACCESS** I

III Metrics & More

Article Recommendations

Supporting Information

ABSTRACT: Discotic polycyclic aromatics have attracted great interest in both fundamental chemistry and material science due to their degenerate frontier orbitals, high molecular symmetry, unique solid-state packing, and ability to bear a certain number of unpaired electrons that can be applied in molecular spintronics and quantum computing. In this work, chemical reduction of hexa-perihexabenzocoronenes, HBC (1) and tBu-HBC (2), as "superbenzenes", has been investigated with K metal in THF solution.



These reactions readily afforded the triply reduced HBC-based products which have been isolated as single-crystalline materials. The X-ray diffraction study confirmed the formation of  $\pi$ -complexes  $[K^+(18\text{-crown-6})(THF)_2][\{K^+(18\text{-crown-6})\}_2(1^{3-})]$  (3) and  $[K^{+}(18\text{-crown-6})(THF)_{2}][\{K^{+}(18\text{-crown-6})\}_{2}(2^{3-})]$  (4). In 3 and 4, two potassium ions were found to bind the central sixmembered rings of 13- and 23- with one potassium counterion remaining solvent-separated from the complexes. A notable geometry distortion of the HBC core upon three-electron acquisition and metal binding was revealed in both complexes. The presence of bulky substituents in 2 affected the coordination and crystal packing of otherwise similar building units in 4 vs 3. The magnetic properties of 4 supported the existence of a well-isolated S = 3/2 ground state of the  $2^{3-}$  triradical in the solid state.

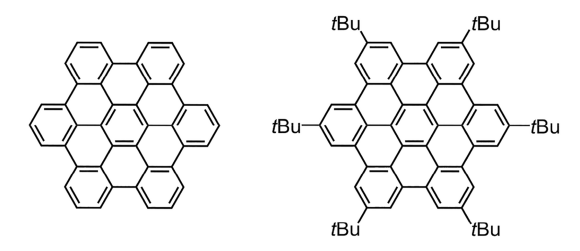
## **■ INTRODUCTION**

The study of triradical compounds has attracted special interest over the decades not only due to their fundamental significance but also due to their attractive materials applications stemming from unique optical, electronic, and magnetic properties.<sup>1,2</sup> Despite their high reactivity, triradicals have been prepared by employing congested  $\pi$ -conjugated scaffolds enabling electron delocalization, as well as by doping with heteroatom centers (e.g., nitrogen and boron) that carry unpaired electrons.<sup>3,4</sup> Without heteroatoms, the preparation of triradicals of polycyclic aromatic hydrocarbons (PAHs) remains challenging, and their investigations have mostly been restricted to computational studies. We have accomplished the structural characterization of the triply reduced bowl-shaped corannulene radicals and confirmed their tendency to self-assemble with multiple alkali-metal ions. 5,6 Magnetic susceptibility measurements supported by theoretical investigations revealed that the doubly degenerate LUMOs of corannulene enabled the formation of monoradicals with two paired and one unpaired electrons. Notably, the downsizing of the intercalated alkali-metal units enabled tuning magnetic interactions in supramolecular sandwiches formed by the triply reduced corannulene.<sup>6</sup> Extension of these studies to highly symmetrical planar PAHs accommodating three unpaired

electrons in three unoccupied orbitals with similar energies would be highly promising.

Among such PAHs, hexa-peri-hexabenzocoronenes (HBCs) feature high molecular symmetries  $(D_{6h})$  and columnar packing structures in the solid state (Scheme 1). The discotic

Scheme 1. Chemical Structures of HBC (1) and tBu-HBC



Received: November 7, 2022 Revised: December 14, 2022 Published: January 9, 2023





hexa-peri-hexabenzocoronene (HBC,  $C_{42}H_{18}$ , 1) was first synthesized by Clar et al. in 1959 and structurally characterized decades later by Goddard et al. X-ray studies proved its perfectly planar geometry, while the rigid and large core of 1 resulted in poor solubility in most organic solvents. To combat this issue, hexa-tert-butylhexa-peri-hexabenzocoronene (tBu-HBC,  $C_{66}H_{66}$ , 2) and other alkyl-substituted HBCs were later synthesized. The improved solubility and nanophase separation of these derivatives gave rise to discopic mesophases with promising charge-transport behavior and with columnar superstructures serving as nanowires.  $^{15-18}$ 

HBCs also show interesting redox and coordination properties, but only a few examples have been reported so far. In 2000, the first stable radical cation of 2,  $[(C_{66}H_{66})_2AsF_6]$ , was prepared and structurally characterized  $^{11}$ via electrochemical oxidation with  $[N(C_4H_9)_4][AsF_6]$ . In 2011, the Weller group reported the preparation and crystal structure of  $[Rh(C_{66}H_{66})(COD)](BAr_4^F)$  (Ar =  $C_6H_3(CF_3)_2$ ) by reacting  $[RhCl(COD)]_2$  and  $Na[BAr^F_4]$  with  ${\bf 2}^{19}$  The reduction study of  ${\bf 2}$  was initiated by us  $^{20}$ using potassium metal. Surprisingly, evidence showed that this highly symmetrical hydrocarbon is capable of accepting up to six electrons upon *in situ* reduction. Moreover, the existence of triradical species was confirmed by solution electron paramagnetic resonance (EPR), whereby spin-forbidden transitions with  $\Delta m_s = 2$  and  $\Delta m_s = 3$ , indicating the quartet ground state, were observed. However, the product was only characterized by in situ EPR and kinetic UV-vis absorption spectroscopy in dilute solution and was never isolated in the crystalline form. Herein, we synthesize the triradical trianions of the unsubstituted HBC 1 and its tBu-functionalized derivative 2, crystallize them with potassium counterions, and provide their first structural characterization by single-crystal X-ray diffraction. Remarkably, the products can be isolated as purephase crystalline materials that are relatively stable under inertgas conditions, enabling their investigation by X-ray powder diffraction and magnetic measurements.

# ■ RESULTS AND DISCUSSION

Prior to the reduction study, 2 was purified by sublimation *in vacuo* at elevated temperatures (see the Supporting Information for details). In contrast, 1 was used as received due to its very limited volatility. The chemical reduction of 1 and 2 with K metal has been carried out in tetrahydrofuran (THF) in the presence of 18-crown-6 ether at room temperature (Scheme 2). The stepwise reduction processes have been monitored by UV—vis absorption spectroscopy to demonstrate distinctive color changes (Figures S1–S4). The solution quickly changed color through deep red (monoanion) and dark brown (dianion) to dark green, which is indicative of the formation of HBC trianions. The resulting triply reduced products have been crystallized by slow diffusion of hexanes into the THF

Scheme 2. Controlled Chemical Reduction of 1 and 2 with K Metal to Afford 3 and 4

1 3.4 eq. K, THF  
18-crown-6  
hexanes 
$$[K^{+}(18-crown-6)(THF)_{2}][\{K^{+}(18-crown-6)\}_{2}(\mathbf{1}^{3-})]$$
 (3)  
3.2 eq. K, THF  
2 18-crown-6  
hexanes  $[K^{+}(18-crown-6)(THF)_{2}][\{K^{+}(18-crown-6)\}_{2}(\mathbf{2}^{3-})]$  (4)

solution. Notably, the UV—vis absorption spectra of crystals dissolved in THF were shown to be comparable to those of the *in situ* generated species (Figures S5 and S6). The crystalline products have been characterized by single-crystal X-ray diffraction analysis as  $[K^+(18\text{-crown-6})(THF)_2][\{K^+(18\text{-crown-6})\}_2(1^{3-})]$  (3) and  $[K^+(18\text{-crown-6})(THF)_2][\{K^+(18\text{-crown-6})\}_2(2^{3-})]$  (4).

In the crystal structure of 3 (Figure 1), the  $1^{3-}$  trianion is sandwiched by two {K<sup>+</sup>(18-crown-6)} cations (there are only two independent K<sup>+</sup> ions due to the symmetry; Figure S8). The K1 ion is asymmetrically bound to the central six-membered ring of  $1^{3-}$ , with the corresponding K–C bond distances in the range 3.156(7)-3.312(7) Å, and is trapped by one 18-crown-6 ether molecule (K–O<sub>crown</sub> 2.781(16)-3.005(15) Å). The K2 ion is fully wrapped by one 18-crown-6 ether (K–O<sub>crown</sub> 2.760(7)-2.819(7) Å) and two THF molecules (K–O<sub>THF</sub> 2.869(15) Å), thus remaining essentially separated from the anionic sandwich.

In the crystal structure of 4 (Figure 2), similarly, two  $\{K^+(18\text{-crown-}6)\}$  cations sandwich the  $2^{3^-}$  trianion with the  $K^+$  ion being symmetrically bound to the central six-membered ring (K–C 3.306(2) Å, Figure S9) and trapped by one 18-crown-6 ether (K– $O_{crown}$  2.811(2)/2.974(2) Å). The K2 ion is fully surrounded by one 18-crown-6 ether (K– $O_{crown}$  2.806(2) Å) and two THF molecules (K– $O_{THF}$  2.757(5) Å). A comparison of two anionic sandwiches shows that the distance of the K<sup>+</sup> ion from the ring centroid in 4 is notably shorter (2.986(2) Å, Figure 2c) than that in 3 (3.023(7) Å, Figure 1c). Unlike our recently reported potassium salt of a triphenylene radical monoanion,  $^{21}$  all K–C and K–O distances are comparable to those previously reported.  $^{21-24}$ 

In the solid-state structures of 3 and 4, the alternating building blocks are aligned as stacked columns (Figure 3 and Figure S10). Notably, the alignment of  $\{K^+(18\text{-crown-}6)(THF)_2\}$  moieties in the columns of 3 is tilted at a 17.0° angle with respect to the plane of  $\mathbf{1}^{3-}$ , while those in 4 are fully "standing up" between the complexed  $[\{K^+(18\text{-crown-}6)\}_2(\mathbf{2}^{3-})]$  units (highlighted by red arrows). This difference may stem from the presence of bulky t-Bu substituents in 4 and results in greater separation between the functionalized HBC decks within and across the columns. For example, the shortest distance between two HBC decks (highlighted in blue) is measured at 6.45 Å in 3 vs 7.71 Å in 4.

The deformation of the HBC cores in 3 and 4 was detected upon three-electron acquisition and evaluated by a comparison of torsion angles and interplane dihedral angles of the triradical species vs neutral parent compounds. According to the torsion angle analysis (Table 1), the edge of the HBC core is only very slightly twisted than the center in both neutral 1 ( $|avg| = 1.0^{\circ}$ ) and 2 (lavgl =  $0.8^{\circ}$ ). After the addition of three electrons, the whole core becomes more distorted in 3 (lavgl =  $4.7^{\circ}$ ) and 4 (l avgl =  $3.7^{\circ}$ ). In 1, the exterior benzene rings (A-E) are only slightly bent in comparison to the reference plane, with a deviation from planarity of  $1.0^{\circ}$  and a symmetry close to  $D_{6h}$ (Table 2). In the triply reduced state (3), the HBC core becomes more bent (avg 4.6°), which is accompanied by a symmetry reduction  $(C_2)$ . In contrast, rings A-E in 2 are asymmetrically bent (avg 5.6°), particularly at rings C (7.6°) and D (6.9°). This is mainly caused by relatively stronger intermolecular forces  $(\pi \cdots \pi \ 3.358(2) \text{ Å, C-H} \cdots \pi \ 2.504(2) -$ 2.731(2) Å) between two tBu-HBC molecules, thus breaking the symmetry to the lowest  $C_1$ . In 4, the dihedral angle is  $3.7^{\circ}$ , forming a wavy-like nanographene unit with a symmetry of Crystal Growth & Design pubs.acs.org/crystal Article

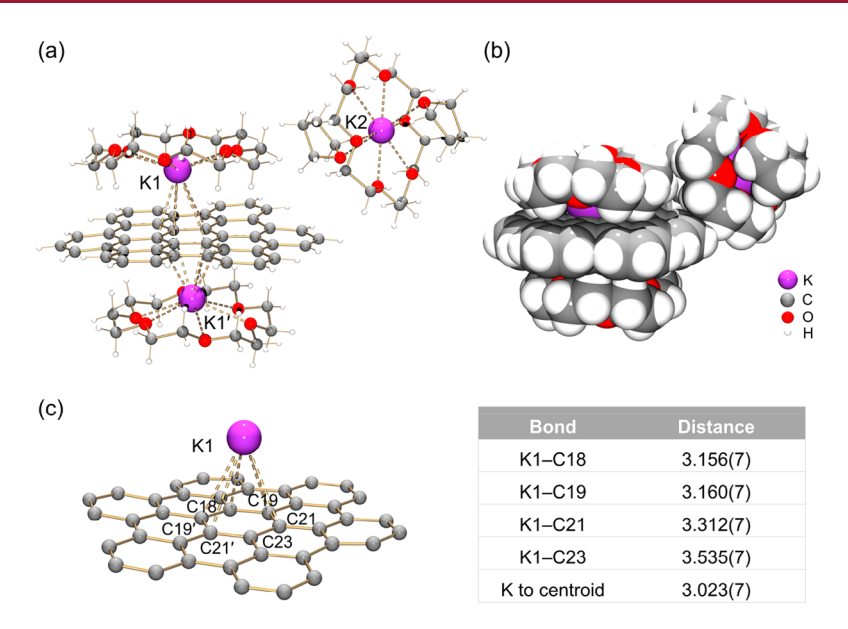


Figure 1. Crystal structure of 3: (a) ball-and-stick and (b) space-filling models and (c) metal coordination in 3 along with a table of distances (Å).

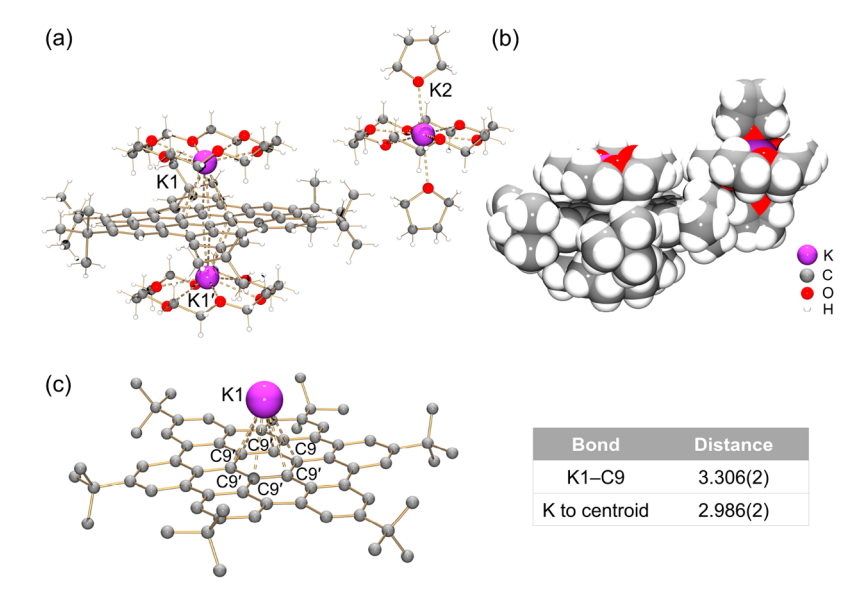


Figure 2. Crystal structure of 4: (a) ball-and-stick and (b) space-filling models and (c) metal coordination in 4 along with a table of distances (Å).

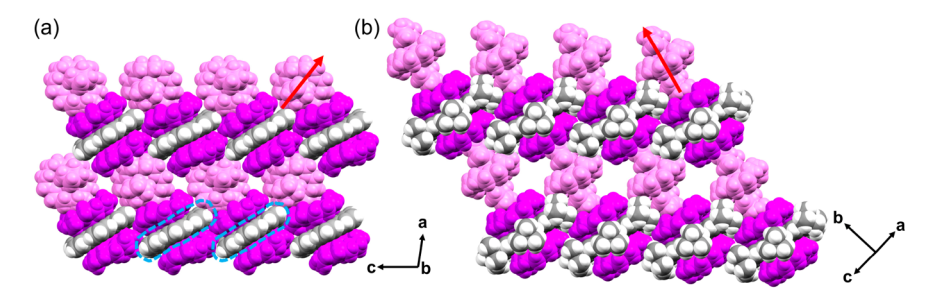


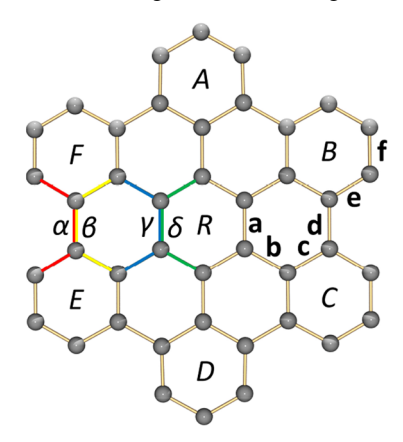
Figure 3. Solid-state packing in (a) 3 and (b) 4, shown as space-filling models. The  $\{K^+(18\text{-crown-}6)(THF)_2\}$  and  $\{K^+(18\text{-crown-}6)\}$  moieties are shown in different shades of purple.

 $D_{3d}$ . In addition, the C-C bonds of rings A-F (c, e, and f) and R (a) are averaged at 1.402(2) and 1.405(2) Å in 1 and 2, respectively. These bonds are elongated to 1.418(11) Å in 3 and 1.421(4) Å in 4 (Table 2). In contrast, the C-C bonds between these rings (b and d) are much longer in the neutral

states (avg 1.454(2) Å) and are noticeably shortened by 0.24 Å (avg 1.430(11) Å) in the triply reduced species. The C–C bond changes are consistent with the resonance structure of 4 drawn in Figure 5, revealing the nature and magnitude of the

Crystal Growth & Design pubs.acs.org/crystal Article

Table 1. Selected Torsion and Dihedral Angles (deg) of HBC Core in 1-4, Along with a Labeling Scheme



angle	17	$2^{14}$	3	4			
Torsion Angles							
$\alpha$	2.0	2.0	-7.5	-4.0			
β	1.2	1.1	-4.6	-6.0			
γ	0.6	0.5	-2.8	-3.2			
$\delta$	0.1	-0.4	-4.0	-1.6			
Dihedral Angles							
A/R	0.2	2.9	4.7	3.7			
B/R	1.2	2.9	4.7	3.7			
C/R	1.5	4.8	4.3	3.7			
D/R	0.2	7.6	4.7	3.7			
E/R	1.2	6.9	4.7	3.7			
F/R	1.5	5.4	4.3	3.7			

Table 2. Average C-C Bond Lengths (Å) of HBC Cores in 1-4

bond	17	<b>2</b> <sup>14</sup>	3	4
a	1.417(2)	1.416(2)	1.436(11)	1.431(4)
b	1.446(2)	1.444(2)	1.429(11)	1.426(4)
c	1.417(2)	1.417(2)	1.434(11)	1.427(4)
d	1.458(2)	1.469(2)	1.432(11)	1.433(4)
e	1.398(2)	1.396(2)	1.421(11)	1.429(4)
f	1.376(2)	1.389(2)	1.380(11)	1.397(4)

electronic delocalization upon chemical reduction and suggesting potential sites for metal coordination.

The isolation of single crystals of 4 (see the Supporting Information for details) enabled the first magnetic property study. The phase purity of the crystalline sample was confirmed by X-ray powder diffraction (Figure S7 and Table S1).

The magnetic susceptibility  $(\chi)$  of 4 was measured on 2.75 mg of a powder sample sealed in a glass capillary. The small amount of the sample and the use of the glass sample holder caused substantial noise in the data (as discussed in the Supporting Information), but the discussion of the magnetic properties provided below remains valid.

The  $\chi T$  product is relatively constant as a function of temperature, around 1.60 emu K mol<sup>-1</sup> (Figure 4), which is close to the value of 1.875 emu K mol<sup>-1</sup> expected for a S=3/2 species. A slight decrease in  $\chi T$  observed below 10 K might be attributed to weak antiferromagnetic intermolecular coupling, although a weak zero-field splitting also can be present (see below). The temperature dependence of inverse magnetic susceptibility (Figure 4, inset) was fitted to the Curie–Weiss

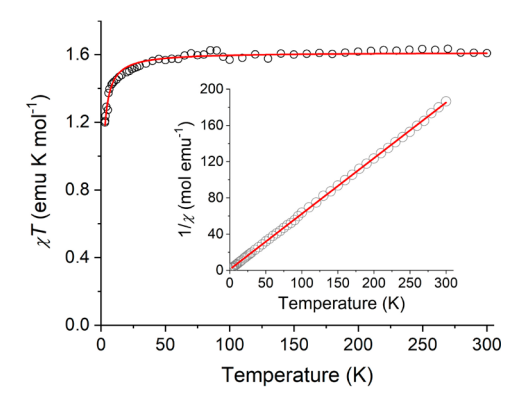


**Figure 4.** Temperature dependence of  $\chi T$  and  $1/\chi$  (inset) measured on a powder sample of 4. The Curie–Weiss fits are shown with solid red lines ( $R^2 = 0.9710$  and 0.9999, respectively).

law,  $1/\chi = (T - \theta)/C$ , to give the best-fit values of the Curie constant, C = 1.628(3) emu·K·mol<sup>-1</sup> and the Weiss constant,  $\theta = -1.6(2)$  K. Assuming that the decrease of the C value from the expected 1.875 emu·K·mol<sup>-1</sup> is caused by the presence of a diamagnetic impurity, we modeled the  $\chi T$  curve by adding a scaling factor (b) to account for this deviation and a molecular field correction (zJ) to account for intermolecular antiferromagnetic interactions at lower temperatures

$$\chi T = \frac{bN\mu_{\rm B}^2 T g^2 S(S+1)}{83k_{\rm B}T - 2(zJ)S(S+1)}$$

where N is Avogardro's number,  $\mu_B$  is the Bohr magneton, and  $k_B$  is Boltzmann's constant. Assuming that the Landé factor g=2.0 and the spin state S=3/2, we obtained the best fit to the experimental  $\chi T$  vs T data with zJ=-0.319(9) cm<sup>-1</sup> and b=0.861(2), equivalent to  $\sim 14$  wt % of diamagnetic impurity (the quality of fit  $R^2=0.9710$ ).

The observed magnetic behavior is in line with the existence of a well-isolated quartet ground state (S=3/2) that is only slightly perturbed by intermolecular antiferromagnetic exchange. The S=3/2 ground state was previously supported by solution EPR studies, which revealed a weak zero-field splitting (ZFS) of such a triradical in solution. The axial ZFS parameter (D) was found to be <0.01 cm<sup>-1</sup>. This value is substantially smaller than the effective molecular field parameter zJ determined above. Thus, we can conclude that the main contribution to zJ stems from intermolecular antiferromagnetic coupling.

The S = 3/2 ground state is in agreement with the ferromagnetic intramolecular coupling between the three localized radicals that follows Ovchinnikov's rules. Indeed, in any of the resonance forms depicted in Figure 5, each pair of radicals is separated by an odd number of  $\pi$ -conjugated carbon atoms, which should result in a parallel arrangement of the spin centers. Similar behavior has been reported recently for aminyl triradicals with a cross-conjugated  $\pi$ -system.<sup>25</sup> In contrast, the loss of conjugation leads to weakening of the intramolecular spin correlations, as was shown for several systems with variable strength and sign of intramolecular magnetic exchange. For example, a pronounced temperature dependence of  $\chi T$  was observed in a series of nitroxide triradicals, due to weaker ferromagnetic exchange that led to the room-temperature  $\chi T$  value being much closer to 1.125 emu K mol<sup>-1</sup>, expected for three noninteracting S = 1/2 centers.<sup>26</sup> A triradical obtained by reduction of a naphthalenediimide

**Figure 5.** Resonance structures of the triradical core of 4, demonstrating the magnetic exchange pathways between the spin centers.

triangle showed antiferromagnetic intramolecular exchange, which led to a spin-frustrated (degenerate) ground-state doublet and a thermally accessible excited-state quartet.<sup>27</sup> Similar observations were reported for a multiphenalenyl triradical.<sup>28</sup> The remarkably stable high-spin ground state of 4 suggests that such triradical anions can be explored further as building blocks for molecule-based magnets.

#### CONCLUSION

In summary, the controlled chemical reduction of HBC (1) and tBu-HBC (2) with K metal has been developed to afford the triradical-based products isolated as the single-phase crystalline solids 3 and 4. Their X-ray structural analysis revealed the formation of two  $\pi$ -complexes in which the central six-membered ring of the triply reduced HBC,  $1^{3-}$  and  $2^{3-}$ respectively, serves as a binding site for complexing two K<sup>+</sup> ions on the opposite faces of HBC. The third cationic moiety is fully wrapped by 18-crown-6 and two THF molecules and forms alternating columnar stacks with the above anionic complexes. The presence of bulky substituents in 2 affects the crystal packing of otherwise similar cationic and anionic building blocks in 4 vs 3. The successful preparation of bulk crystalline products enables the first magnetic measurements which support the existence of the S = 3/2 state for the triradical 23- in the solid state and suggest that such species can be used as building blocks for molecule-based magnets.

Hexabenzocoronene has played an important role in attempts at making PAHs larger and larger en route to nanographenes. Furthermore, adding the spin degree of freedom to nanographene and graphene nanoribbon is important in developing complex circuitry. Synthesizing stable spin-bearing nanographenes will therefore become more and more important for single-molecule spintronics and quantum computing nanotechnologies.

## ASSOCIATED CONTENT

## Supporting Information

The Supporting Information is available free of charge at https://pubs.acs.org/doi/10.1021/acs.cgd.2c01294.

Experimental details, UV-vis spectra, single crystal and powder X-ray diffraction data, and magnetic data (PDF)

#### **Accession Codes**

CCDC 2217109-2217110 contain the supplementary crystallographic data for this paper. These data can be obtained free of charge via www.ccdc.cam.ac.uk/data\_request/cif, or by emailing data request@ccdc.cam.ac.uk, or by contacting The

Cambridge Crystallographic Data Centre, 12 Union Road, Cambridge CB2 1EZ, UK; fax: +44 1223 336033.

# AUTHOR INFORMATION

#### **Corresponding Authors**

Marina A. Petrukhina — Department of Chemistry, University at Albany, State University of New York, Albany, New York 12222, United States; orcid.org/0000-0003-0221-7900; Email: mpetrukhina@albany.edu

Michael Shatruk — Department of Chemistry and Biochemistry, Florida State University, Tallahassee, Florida 32306-4390, United States; orcid.org/0000-0002-2883-4694; Email: shatruk@chem.fsu.edu

#### **Authors**

Zheng Zhou — Department of Chemistry, University at Albany, State University of New York, Albany, New York 12222, United States; Interdisciplinary Materials Research Center, School of Materials Science and Engineering, Tongji University, Shanghai 201804, People's Republic of China; orcid.org/0000-0001-8905-9663

Zheng Wei – Department of Chemistry, University at Albany, State University of New York, Albany, New York 12222, United States

Xuelin Yao — Max Planck Institute for Polymer Research, 55128 Mainz, Germany; orcid.org/0000-0002-4287-6073

Xiao-Ye Wang — Max Planck Institute for Polymer Research, 55128 Mainz, Germany; State Key Laboratory of Elemento-Organic Chemistry, College of Chemistry, Nankai University, Tianjin 300071, People's Republic of China; orcid.org/0000-0003-3540-0277

Klaus Müllen – Max Planck Institute for Polymer Research, 55128 Mainz, Germany; orcid.org/0000-0001-6630-

Minyoung Jo – Department of Chemistry and Biochemistry, Florida State University, Tallahassee, Florida 32306-4390, United States

Complete contact information is available at: https://pubs.acs.org/10.1021/acs.cgd.2c01294

#### **Notes**

The authors declare no competing financial interest.

#### ACKNOWLEDGMENTS

Financial support from the U.S. National Science Foundation is gratefully acknowledged (CHE-2003411 by M.A.P. and CHE-1955754 by M.S.).

## **■** REFERENCES

- (1) Gerson, F.; Huber, W. Novel Chemical Species: Radical Trianions. Acc. Chem. Res. 1987, 20, 85–90.
- (2) Krylov, A. I. Triradicals. J. Phys. Chem. B 2005, 109, 10638–10645.
- (3) Dulog, L.; Kim, J. S. A Stable Triradical Compound and its Unusual Magnetic Properties. *Angew. Chem., Int. Ed.* **1990**, 29, 415–417
- (4) Winkler, M.; Sander, W. Triradicals. Acc. Chem. Res. 2014, 47,
- (5) Zabula, A. V.; Spisak, S. N.; Filatov, A. S.; Rogachev, A. Yu.; Clérac, R.; Petrukhina, M. A. Supramolecular Trap for a Transient Corannulene Trianion. *Chem. Sci.* **2016**, *7*, 1954–1961.
- (6) Spisak, S. N.; Rogachev, A. Yu.; Zabula, A. V.; Filatov, A. S.; Clérac, R.; Petrukhina, M. A. Tuning the Separation and Coupling of

- Corannulene Trianion-Radicals through Sizable Alkali Metal Belts. *Chem. Sci.* **2017**, *8*, 3137–3145.
- (7) Clar, E.; Ironside, C. T.; Zander, M. The Electronic Interaction between Benzenoid Rings in Condensed Aromatic Hydrocarbons. 1:12–2:3–4:5–6:7–8:9–10:11-Hexabenzocoronene, 1:2–3:4–5:6–10:11-Tetrabenzoanthanthrene, and 4:5–6:7–11:12–13:14-Tetrabenzoperopyrene. *J. Chem. Soc.* 1959, 142–147.
- (8) Goddard, R.; Haenel, M. W.; Herndon, W. C.; Krueger, C.; Zander, M. Crystallization of Large Planar Polycyclic Aromatic Hydrocarbons: The Molecular and Crystal Structures of Hexabenzo-[bc,ef,hi,kl,no,qr]coronene and Benzo[1,2,3-bc:4,5,6-b'c']dicoronene. J. Am. Chem. Soc. 1995, 117, 30–41.
- (9) Herwig, P.; Kayser, C. W.; Müllen, K.; Spiess, H. W. Columnar Mesophases of Alkylated Hexa-*peri*-hexabenzocoronenes with Remarkably Large Phase Widths. *Adv. Mater.* **1996**, *8*, 510–513.
- (10) Brown, S. P.; Schnell, I.; Brand, J. D.; Müllen, K.; Spiess, H. W. An Investigation of  $\pi \pi$  Packing in a Columnar Hexabenzocoronene by Fast Magic-Angle Spinning and Double-Quantum <sup>1</sup>H Solid-State NMR Spectroscopy. *J. Am. Chem. Soc.* **1999**, *121*, 6712–6718.
- (11) Herwig, P. T.; Enkelmann, V.; Schmelz, O.; Müllen, K. Synthesis and Structural Characterization of Hexa-tert-butyl-hexa-peri-hexabenzocoronene, Its Radical Cation Salt and Its Tricarbonylchromium Complex. Chem. Eur. J. 2000, 6, 1834–1839.
- (12) Liu, C.-y.; Fechtenkötter, A.; Watson, M. D.; Müllen, K.; Bard, A. J. Room Temperature Discotic Liquid Crystalline Thin Films of Hexa-peri-hexabenzocoronene: Synthesis and Optoelectronic Properties. Chem. Mater. 2003, 15, 124–130.
- (13) Sadhukhan, S. K.; Viala, C.; Gourdon, A. Syntheses of Hexabenzocoronene Derivatives. *Synthesis* **2003**, 1521–1525.
- (14) Zhai, L.; Shukla, R.; Rathore, R. Oxidative C-C Bond Formation (Scholl Reaction) with DDQ as an Efficient and Easily Recyclable Oxidant. *Org. Lett.* **2009**, *11*, 3474–3477.
- (15) Schmidt-Mende, L.; Fechtenkötter, A.; Müllen, K.; Moons, E.; Friend, R. H.; MacKenzie, J. D. Self-Organized Discotic Liquid Crystals for High-Efficiency Organic Photovoltaics. *Science* **2001**, 293, 1119.
- (16) Pisula, W.; Tomović, Ž.; El Hamaoui, B.; Watson, M. D.; Pakula, T.; Müllen, K. Control of the Homeotropic Order of Discotic Hexa-peri-hexabenzocoronenes. *Adv. Funct. Mater.* **2005**, *15*, 893–904.
- (17) Wakikawa, Y.; Ikoma, T.; Yamamoto, Y.; Fukushima, T.; Akiyama, K. Temperature Dependence of Magnetophotoconductance in One-Dimensional Molecular Assembly of Hexabenzocoronene. *ACS Omega* **2017**, *2*, 3260–3266.
- (18) van de Craats, A. M.; Warman, J. M.; Müllen, K.; Geerts, Y.; Brand, J. D. Rapid Charge Transport Along Self-Assembling Graphitic Nanowires. *Adv. Mater.* **1998**, *10*, 36–38.
- (19) Woolf, A.; Chaplin, A. B.; McGrady, J. E.; Alibadi, M. A. M.; Rees, N.; Draper, S.; Murphy, F.; Weller, A. S. {Rh(PiBu<sub>3</sub>)<sub>2</sub>}\* Fragments Ligated to Arenes: From Benzene to Polyaromatic Hydrocarbons, Part I An Experimental Approach. *Eur. J. Inorg. Chem.* **2011**, 2011, 1614–1625.
- (20) Gherghel, L.; Brand, J. D.; Baumgarten, M.; Müllen, K. Exceptional Triplet and Quartet States in Highly Charged Hexabenzocoronenes. *J. Am. Chem. Soc.* **1999**, *121*, 8104–8105.
- (21) Zhou, Z.; Üngör, Ö.; Wei, Z.; Shatruk, M.; Tsybizova, A.; Gershoni-Poranne, R.; Petrukhina, M. A. Tuning Magnetic Interactions Between Triphenylene Radicals by Variation of Crystal Packing in Structures with Alkali Metal Counterions. *Inorg. Chem.* **2021**, *60*, 14844–14853.
- (22) Zhou, Z.; Wei, Z.; Hirao, T.; Amaya, T.; Petrukhina, M. A. Structural Consequences of Two-Fold Deprotonation of Sumanene: Embedding Two Cp-rings into a Nonplanar Carbon Framework. *Organometallics* **2021**, *40*, 2023–2026.
- (23) Zhou, Z.; Wei, Z.; Ikemoto, K.; Sato, S.; Isobe, H.; Petrukhina, M. A. Chemical Reduction of Nanosized [6]Cyclo-2,7-naphthylene Macrocycle. *Angew. Chem., Int. Ed.* **2021**, *60*, 11201–11205.
- (24) Zhou, Z.; Egger, D. T.; Hu, C.; Pennachio, M.; Wei, Z.; Kawade, R. K.; Üngör, Ö.; Gershoni-Poranne, R.; Petrukhina, M. A.;

- Alabugin, I. V. Localized Antiaromaticity Hotspot Drives Reductive Dehydrogenative Cyclizations in Bis- and Mono-Helicenes. *J. Am. Chem. Soc.* **2022**, *144*, 12321–12338.
- (25) Zhang, H.; Pink, M.; Wang, Y.; Rajca, S.; Rajca, A. High-Spin *S* = 3/2 Ground-State Aminyl Triradicals: Toward High-Spin Oligo-Aza Nanographenes. *J. Am. Chem. Soc.* **2022**, *144*, 19576–19591.
- (26) Tanaka, M.; Matsuda, K.; Itoh, T.; Iwamura, H. Syntheses and Magnetic Properties of Stable Organic Triradicals with Quartet Ground States Consisting of Different Nitroxide Radicals. *J. Am. Chem. Soc.* **1998**, *120*, 7168–7173.
- (27) Wu, Y.; Krzyaniak, M. D.; Stoddart, J. F.; Wasielewski, M. R. Spin Frustration in the Triradical Trianion of a Naphthalenediimide Molecular Triangle. *J. Am. Chem. Soc.* **2017**, *139*, 2948–2951.
- (28) Kodama, T.; Aoba, M.; Hirao, Y.; Rivero, S. M.; Casado, J.; Kubo, T. Molecular and Spin Structures of a Through-Space Conjugated Triradical System. *Angew. Chem., Int. Ed.* **2022**, *61*, e202200688.
- (29) Sugawara, T.; Matsushita, M. M. Spintronics in Organic  $\pi$ -Electronic Systems. *J. Mater. Chem.* **2009**, *19*, 1738–1753.
- (30) Choudhuri, I.; Bhauriyal, P.; Pathak, B. Recent Advances in Graphene-like 2D Materials for Spintronics Applications. *Chem. Mater.* **2019**, *31*, 8260–8285.
- (31) Rabelo, R.; Stiriba, S.-E.; Cangussu, D.; Pereira, C.; Moliner, N.; Ruiz-García, R.; Cano, J.; Faus, J.; Journaux, Y.; Julve, M. When Molecular Magnetism Meets Supramolecular Chemistry: Multifunctional and Multiresponsive Dicopper(II) Metallacyclophanes as Proof-of-Concept for Single-Molecule Spintronics and Quantum Computing Technologies E. Magnetochemistry 2020, 6, 69.
- (32) Yuste, C.; Castellano, M.; Ferrando-Soria, J.; Stiriba, S.-E.; Marino, N.; Julve, M.; Lloret, F.; Ruiz-García, R.; Cano, J. Review: From Computational Design to the Synthesis of Molecular Magnetic Wires for Single-Molecule Spintronics and Quantum Computing Nanotechnologies. *J. Coord. Chem.* **2022**, *75*, 2359–2383.

# **□** Recommended by ACS

## **Singlet Fission and Aromaticity**

Amnon Stanger.

OCTOBER 24, 2022

THE JOURNAL OF PHYSICAL CHEMISTRY A

READ 🗹

# **Electrostatic Potential for Exploring Electron Delocalization** in Infinitenes, Circulenes, and Nanobelts

Puthannur K. Anjalikrishna, Cherumuttathu H. Suresh, et al.

MARCH 23, 2023

THE JOURNAL OF ORGANIC CHEMISTRY

READ 🗹

# Planar Four-Membered Diboron Actinide Compound with Double Möbius Aromaticity

Xuhui Lin, Yirong Mo, et al.

MARCH 28, 2023

JOURNAL OF THE AMERICAN CHEMICAL SOCIETY

READ 🗹

# Dibenzotropylium-Capped Orthogonal Geometry Enabling Isolation and Examination of a Series of Hydrocarbons with Multiple $14\pi$ -Aromatic Units

Yuki Hayashi, Yusuke Ishigaki, et al.

JANUARY 06, 2023

JOURNAL OF THE AMERICAN CHEMICAL SOCIETY

READ 🗹

Get More Suggestions >